Pattern formation in the instability of a vicinal surface by the drift of adatoms

Masahide Sato[1,2] and Makio Uwaha[1]
[1]*Department of Physics, Nagoya University, Furo-cho, Chikusa-ku, Nagoya 464-8602, Japan*
[2]*Computer Center, Gakushuin University, 1-5-1 Mejiro, Toshima-ku, Tokyo 171-8588, Japan*
(Received 26 April 1999; revised manuscript received 21 June 1999)

We study the behavior of steps in a vicinal face with drift of adsorbed atoms (adatoms) by an external field. When the drift is in the downhill direction and its velocity exceeds critical values, v_c^x and v_c^y, the vicinal face is linearly unstable to long-wavelength fluctuations parallel and/or perpendicular to the steps. By taking the continuum limit of the step-flow model, we derive an anisotropic Kuramoto-Sivashinsky equation with propagative terms, which describes the motion of an unstable vicinal face. Its numerical solution shows ripples or a zigzag pattern expected from the linear analysis. Nonlinearity becomes important in the late stage and, depending on the condition, various patterns are formed: regular step bunches, a hill and valley structure tilted from the initial step direction, mounds, and a chaotic pattern. [S1063-651X(99)03612-0]

PACS number(s): 81.10.Aj, 05.70.Ln, 47.20.Hw, 05.45.−a

I. INTRODUCTION

Morphological instability in a vicinal face is a result of the two linear instabilities of steps: wandering and bunching. When a train of steps encounters the wandering (or bunching) instability, ripples perpendicular to (or parallel to) the steps occur. These instabilities are induced by the asymmetry of the surface diffusion field of adsorbed atoms (adatoms). Typical causes of the asymmetry are the Ehrlich-Schwoebel (ES) effect [1–5] and the drift of adatoms by an external field [6–14].

When a vicinal face is grown by molecular-beam eptaxiy (MBE), the formation of large bunches is observed [15–18]. This morphological instability is probably caused by the ES effect. When adatoms attach to the step easier from the lower terrace, the wandering (or bunching) occurs in growth (or in sublimation) when supersaturation (or undersaturation) exceeds a critical value [3–5]. When the ES effect is in the opposite sign, the bunching instability occurs in growth. Since the two instabilities do not occur simultaneously, the initial stage of the instabilities can be studied with one-dimensional models. Two-dimensional effects influence the surface morphology in a late stage of instability [4,19,20]. When the wandering instability occurs, ripples perpendicular to the steps are produced at the initial stage as expected from the linear analysis. At a late stage the unstable vicinal face shows a chaotic pattern or a moundlike structure by the wandering of the steps [20].

In a Si(111) vicinal surface, the bunching instability is observed when the specimen is heated by direct electric current [21–24]. The cause of the instability is the drift of adatoms induced by the electric current. Adatoms have an effective charge and encounter a force proportional to the external field [25]. When the bunches are almost straight as observed in several experiments [22,23], essential features are explained by the one-dimensional step-flow model [12–14], However, it has been shown that the drift also causes the wandering instability [10,11] at the same time. If this happens, the produced pattern should be more complicated than that with the ES effect.

In this paper we study two-dimensional motion of steps in a vicinal surface with the drift of adatoms. In order to describe the pattern of the surface, we derive a nonlinear evolution equation by taking the continuum limit of the step-flow model. Numerical integration of the equation is carried out for two situations: the vicinal face is unstable to only bunching and to both bunching and wandering.

II. MODEL

We use the step-flow model of Stoyanov [6–11]. We set the y axis in the downhill direction and the x axis along the steps. Adatoms diffuse on a terrace with the diffusion constant D_s and drift with a velocity v in the downhill direction before they evaporate with the lifetime τ. The diffusion equation of adatom density is given by

$$\frac{\partial c}{\partial t} = D_s \nabla^2 c - v \frac{\partial c}{\partial y} - \frac{1}{\tau} c. \tag{1}$$

The current of adatoms at the nth step is proportional to the difference of adatom density at the step and its equilibrium value c_n,

$$\pm D_s \hat{\boldsymbol{n}} \cdot \nabla c|_{\pm} \mp v c|_{\pm} = K_{\pm}(c|_{\pm} - c_n), \tag{2}$$

where $\hat{\boldsymbol{n}}$ is the unit vector normal to the step, $K_{\pm}$ are the kinetic coefficients, and the suffix $+$ $(-)$ indicates the lower (upper) terrace. The different values of K_+ and K_- imply the ES effect [2,3]. In the following, we neglect the ES effect and set $K_{\pm} = K$ for simplicity. When the neighboring steps with a distance l interact with the repulsive potential $A/l^{-\nu}$, the equilibrium adatom density at the nth step is given by

$$c_n = c_{\mathrm{eq}}^0 \left[1 - \frac{\Omega \tilde{\beta}}{k_{\mathrm{B}} T} \kappa + \frac{\nu \Omega A}{k_{\mathrm{B}} T} \sum_{m=n\pm 1} \frac{1}{(y_n - y_m)^{\nu+1}} \right], \tag{3}$$

where c_{eq}^0 is the equilibrium adatom density of an isolated straight step, y_n is the position of the nth step, $\tilde{\beta}$ is the step stiffness, Ω is the atomic area, and κ is the step curvature.

We set $\nu=2$, which corresponds to the elastic repulsion. By solving Eq. (1) with Eq. (2) in the quasistatic approximation ($\partial c/\partial t=0$), we can determine the adatom density. The position of the nth step is given by the deviation $\zeta_n(x,t)$ from the ideal vicinal growth as $y_n=v_0(l)t+nl+\zeta_n(x,t)$. Time evolution of the fluctuation ζ_n is given by

$$\frac{1}{\sqrt{1+(\partial\zeta_n/\partial x)^2}}\left(v_0+\frac{\partial\zeta_n}{\partial t}\right)$$
$$=\Omega(D_s\hat{\boldsymbol{n}}\cdot\boldsymbol{\nabla}c|_+-vc|_+)-\Omega(D_s\hat{\boldsymbol{n}}\cdot\boldsymbol{\nabla}c|_--vc|_-). \quad (4)$$

III. LINEAR ANALYSIS

When the drift velocity is smaller than the characteristic velocity of the surface diffusion, $v<D_s/x_s$ ($x_s\equiv\sqrt{D_s\tau}$ is the surface diffusion length), the linear dispersion relation is obtained for a small perturbation, $\zeta_n(x,t)=\zeta_1\exp(iqx+iknl+\omega t)$, with the wavelength larger than x_s as

$$\omega(k,q)=i\alpha_1k+\alpha_2k^2+i\alpha_3k^3+\alpha_4k^4+\beta_2q^2+\beta_4q^4+i\mu_1kq^2+\mu_2k^2q^2, \quad (5)$$

where the coefficients are

$$\frac{\alpha_1}{\Omega D_sc_{\rm eq}^0}=-\frac{l}{x_s^2},$$

$$\frac{\alpha_2}{\Omega D_sc_{\rm eq}^0}=\frac{vl^2K}{2D_s^2}-\frac{6\Omega A}{k_{\rm B}Tlx_s^2},$$

$$\frac{\alpha_3}{\Omega D_sc_{\rm eq}^0}=-\frac{l^3}{6x_s^2}-\frac{3\Omega Avk}{k_{\rm B}TD_s^2},$$

$$\frac{\alpha_4}{\Omega D_sc_{\rm eq}^0}=-\frac{vl^4K}{24D_s^2}-\frac{3\Omega AK}{k_{\rm B}TD_s}, \quad (6)$$

$$\frac{\beta_2}{\Omega D_sc_{\rm eq}^0}=\frac{vl}{D_s}-\frac{\Omega\tilde{\beta}l}{k_{\rm B}Tx_s},$$

$$\frac{\beta_4}{\Omega D_sc_{\rm eq}^0}=-\frac{\Omega\tilde{\beta}l}{k_{\rm B}T},$$

$$\frac{\mu_1}{\Omega D_sc_{\rm eq}^0}=\frac{D_sl^2}{2Kx_s^2}+\frac{\Omega\tilde{\beta}vl^2K}{2k_{\rm B}TD_s^2},$$

$$\frac{\mu_2}{\Omega D_sc_{\rm eq}^0}=-\frac{\Omega\tilde{\beta}K}{k_{\rm B}TD_s}-\frac{6\Omega A}{k_{\rm B}Tl}-\frac{vl^3}{4D_s}.$$

The real part of Eq. (5) is the growth rate of the perturbation. The first line in Eq. (5) is the dispersion representing the bunching instability of straight steps [9] and the second line is that representing the wandering instability of an in-phase mode. Since α_4 and β_4 are always negative, the vicinal face is stable at short wavelengths. The stability at a long wavelength is determined by α_2 and β_2. When the drift velocity exceeds the critical value v_c^x (or v_c^y), β_2 (or α_2) becomes positive and the vicinal face is unstable to the fluctuation parallel to (or perpendicular to) the step. The critical drift velocities are given by [26]

$$v_c^y=\frac{12D_s^2\Omega A}{Kx_s^2k_{\rm B}Tl^3}, \quad v_c^x=\frac{\Omega\tilde{\beta}D_s}{k_{\rm B}Tx_s^2}. \quad (7)$$

With decreasing the step distance, v_c^y increases because of stronger repulsion and the vicinal face is more stable to the bunching instability while v_c^x is independent of the step distance.

The imaginary part of Eq. (5) gives the propagation speed of the perturbation. With a finite surface diffusion length (in a nonconserved system), the most dominant term in the imaginary part is $i\alpha_1k$ near the threshold of the instability. Then the propagation velocity is independent of the wave vector of the fluctuation. The wave pattern of the fluctuation shifts to the downhill direction with the velocity $V_y=\Omega D_sc_{\rm eq}^0l/x_s^2$.

IV. NONLINEAR EVOLUTION EQUATION

The linear analysis predicts only the beginning of the instability. In order to investigate the time evolution of $\zeta(x,y,t)$ [27], we take account of nonlinear effects arising from the fluctuation of large amplitude. Near the threshold of the instability, a nonlinear evolution equation can be derived systematically by the reductive perturbation method [28]. Here we derive the nonlinear equation by considering the symmetry of the system. The linear part of the evolution equation is obtained by replacing ω, ik, and iq with $\partial/\partial t$, $\partial/\partial y$, and $\partial/\partial x$. Since the vicinal face has the translational symmetry and the inversion symmetry in the x direction, the expected nonlinear terms are ζ_x^2, ζ_y^2, $\zeta_{xx}\zeta_y$, ζ_{xx}^2, $\zeta_{xx}\zeta_{yy}$, ... The wavelength of growing fluctuation is long near the threshold of instability and the most important terms are $\gamma\zeta_x^2$ and $\lambda\zeta_y^2$.

The coefficient γ is obtained by inspecting the velocity of the straight step tilted from the x axis [29]. The normal velocity of the step is a function of the step distance. When the step is tilted with an angle θ, the step distance is $l\cos\theta$ so that it moves in the y direction with the velocity

$$\frac{v_0(l\cos\theta)}{\cos\theta}\approx v_0+\frac{[v_0(l)-v_0'(l)l]}{2}\zeta_x^2. \quad (8)$$

Since the extra term $[v_0(l)-v_0'(l)l]\zeta_x^2/2$ is the origin of the nonlinearity, we can set

$$\gamma=\frac{v_0(l)-v_0'(l)l}{2}. \quad (9)$$

Also the other coefficient λ is obtained from the velocity of the straight step with a change of the step distance. The local step distance is given by $l+(\zeta_{n+1}-\zeta_n)\approx l(1+\zeta_y)$ in the continuum limit of the step number n. The velocity of the straight step is

$$v_0(l+l\zeta_y)\approx v_0(l)+v_0'(l)l\zeta_y+\frac{v_0''(l)l^2}{2}\zeta_y^2. \tag{10}$$

The second term corresponds to $i\alpha_1 k$ in Eq. (5) and the third term is the nonlinear term in the evolution equation:

$$\lambda=\frac{v_0''(l)l^2}{2}. \tag{11}$$

When we take only the lowest order in l, we find

$$\gamma=-\frac{\lambda}{2}=-\frac{c_{\rm eq}^0 D_s}{2KD_s^2x_s^2}\left(\frac{1}{x_s^2}+\frac{K^2}{D_s^2}\right)l^2. \tag{12}$$

The signs of the nonlinear terms, γ and λ, are different [30] and independent of the drift of adatoms. By taking account of Eq. (12), the nonlinear evolution equation is given by

$$\frac{\partial\zeta}{\partial t}=\alpha_1\frac{\partial\zeta}{\partial y}-\alpha_2\frac{\partial^2\zeta}{\partial y^2}-\alpha_3\frac{\partial^3\zeta}{\partial y^3}+\alpha_4\frac{\partial^4\zeta}{\partial y^4}-\beta_2\frac{\partial^2\zeta}{\partial x^2}+\beta_4\frac{\partial^4\zeta}{\partial x^4}$$
$$-\mu_1\frac{\partial^3\zeta}{\partial x^2\partial y}+\mu_2\frac{\partial^4\zeta}{\partial x^2\partial y^2}+\lambda\left(\frac{\partial\zeta}{\partial y}\right)^2-\frac{\lambda}{2}\left(\frac{\partial\zeta}{\partial x}\right)^2. \tag{13}$$

Strictly speaking, Eq. (13) is valid only near the threshold of the two instabilities. However, the form of this equation is determined by the symmetry of the system and by the fact that long-wavelength modes are relevant. Therefore, we will use it for a qualitative description beyond its justifiability. If $\alpha_3=\mu_1=0$ and $\alpha_4=\beta_4=\mu_2/2$ ($\alpha_1\zeta_x$ vanishes with the Galileian transformation, $y\to y+\alpha_1 t$), Eq. (13) is the anisotropic Kuramoto-Sivashinsky equation studied by Rost and Krug [32].

V. NUMERICAL CALCULATION

We investigate the pattern produced by Eq. (13) by carrying out numerical integration of the differential equation. We discretize $H(X,Y,T)$ as $H(i,j,T)$, where $i,j=1,2,\ldots,L(=128)$, and replace the derivatives with x and y to the finite difference [31]. We solve Eq. (13) by using the Runge-Kutta method.

Case I: $v_c^y<v<v_c^x$. The vicinal face is linearly unstable only in the y direction. Since the vicinal face is linearly stable along the step, ζ_{xxxx} is irrelevant. For simplicity, we neglect ζ_{xyy} and ζ_{xxyy}. By using the scaled variables,

$$Y=\sqrt{\frac{\alpha_2}{|\alpha_4|}}(y+\alpha_1 t),\quad X=\sqrt{\frac{2\alpha_2}{|\alpha_4|}}x,$$
$$T=\frac{\alpha_2^2}{|\alpha_4|}t,\quad H=\frac{a\alpha_2}{l\lambda}\zeta, \tag{14}$$

where H is actually a dimensionless fluctuation of the surface height, and dimensionless parameters

$$\delta_1=\sqrt{\frac{\alpha_3^2}{\alpha_2|\alpha_4|}},\quad \delta_2=\left|\frac{2\beta_2}{\alpha_2}\right|, \tag{15}$$

the evolution equation is given by

$$\frac{\partial H}{\partial T}=-\frac{\partial^2 H}{\partial Y^2}-\delta_1\frac{\partial^3 H}{\partial Y^3}-\frac{\partial^4 H}{\partial Y^4}+\delta_2\frac{\partial^2 H}{\partial X^2}+\left(\frac{\partial H}{\partial Y}\right)^2-\left(\frac{\partial H}{\partial X}\right)^2. \tag{16}$$

Near the threshold of the bunching instability, δ_1 and δ_2 are large since α_2 is small. Figure 1 shows snapshots of a solution of Eq. (16) for $\delta_1=1$ and $\delta_2=1$. The initial condition is $H(X,Y,0)\approx 0$ with random small-amplitude fluctuations, and the boundary condition is periodic. The difference of brightness represents the difference of the surface height: the dark is low and the bright is high. The ripple structure parallel to the x direction, which appears at the initial stage, coarsens considerably and shows slight angular crests at the middle stage. At the late stage the ripples become straight and the pattern in the y direction is not symmetric due to the effect of H_{YYY}. If $\delta_1=0$, the ripple pattern has inversion symmetry in the y direction. The coarsening does not proceed much and the fluctuation of ripples in the x direction becomes larger as shown in Fig. 2. Since the form of Eq. (16) is determined by the symmetry of the system, Eq. (16) also describes the bunching by the ES effect. The forms of the bunches in Refs. [15] and [16] are similar to Fig. 1.

Case II: $v_c^x<v<v_c^y$. The vicinal face is linearly unstable only in the x direction. This case is equivalent to the wandering by the ES effect, which has been studied by Pierre-Louis and Misbah [20]. They carried out numerical integration of the nonlinear evolution equation,

$$\frac{\partial H}{\partial T}=\tilde{\eta}_2\frac{\partial^3 H}{\partial Y\partial X^2}+\frac{\partial^2 H}{\partial Y^2}-\frac{\partial^2 H}{\partial X^2}-\frac{\partial^4 H}{\partial X^4}+\left(\frac{\partial H}{\partial X}\right)^2, \tag{17}$$

where the irrelevant terms H_{YYY}, H_{YYYY}, and the nonlinear term H_Y^2 were neglected and the lowest-order propagative term H_{XXY} was taken into account. At the initial stage, ripples perpendicular to the steps appear as expected from the linear analysis and develop without coarsening. The behavior at a late stage depends on the strength of the propagative term $\tilde{\eta}_2$. With a small $\tilde{\eta}_2$, the ripples are torn off and the moundlike structure is produced. With a large $\tilde{\eta}_2$, the destabilized ripple structure shows a chaotic behavior.

Case III: $v_c^y<v_c^x<v$. The vicinal face is linearly unstable in both directions. Then $\delta_3 H_{XXXX}$ ($\delta_3=4|\beta_4/\alpha_4|$) is added to Eq. (16),

$$\frac{\partial H}{\partial T}=-\frac{\partial^2 H}{\partial Y^2}-\delta_1\frac{\partial^3 H}{\partial Y^3}-\frac{\partial^4 H}{\partial Y^4}-\delta_2\frac{\partial^2 H}{\partial X^2}$$
$$-\delta_3\frac{\partial^4 H}{\partial X^4}+\left(\frac{\partial H}{\partial Y}\right)^2-\left(\frac{\partial H}{\partial X}\right)^2. \tag{18}$$

When v is near v_c^x, δ_2 is a small parameter. Figure 3 shows a snapshot of a solution for $\delta_1=1$, $\delta_2=0.2$, and $\delta_3=1$. At the initial stage a zigzag pattern is produced. Later as the amplitude increases, the pattern changes drastically. The ripples are now straightened and form an irregular striation parallel to $y=x$ or $y=-x$. Two orthogonal regions coexist, but one has disappeared in the late stage in Fig. 3 because of

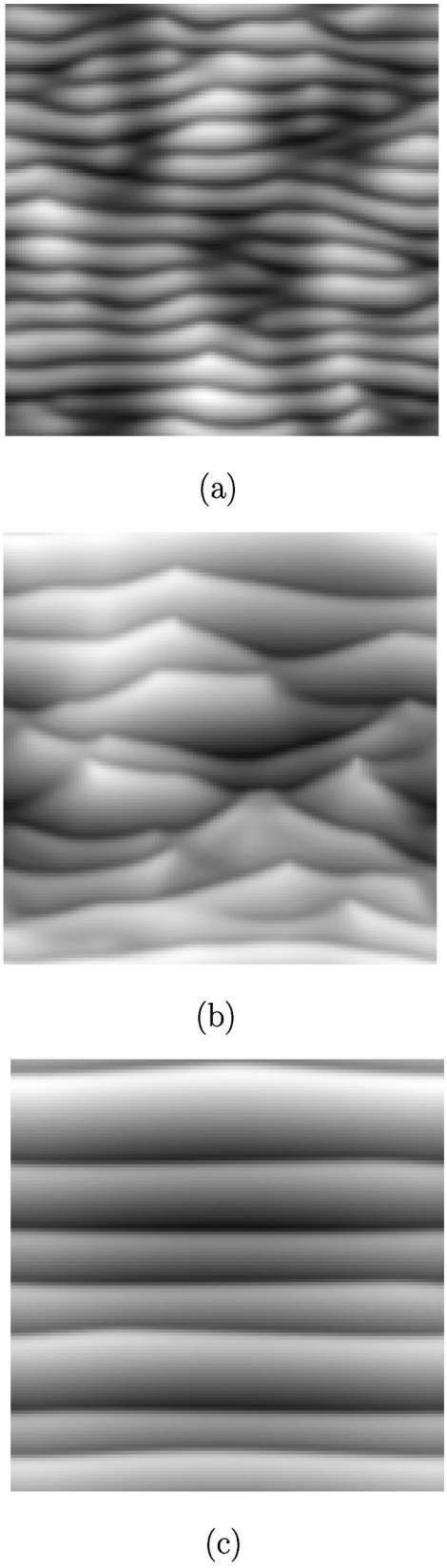

FIG. 1. Snapshots of a solution of Eq. (16) with $\delta_1=\delta_2=1$ at (a) $T=40$, (b) $T=100$, and (c) $T=400$. The system size is 128×128 with the periodic boundary condition.

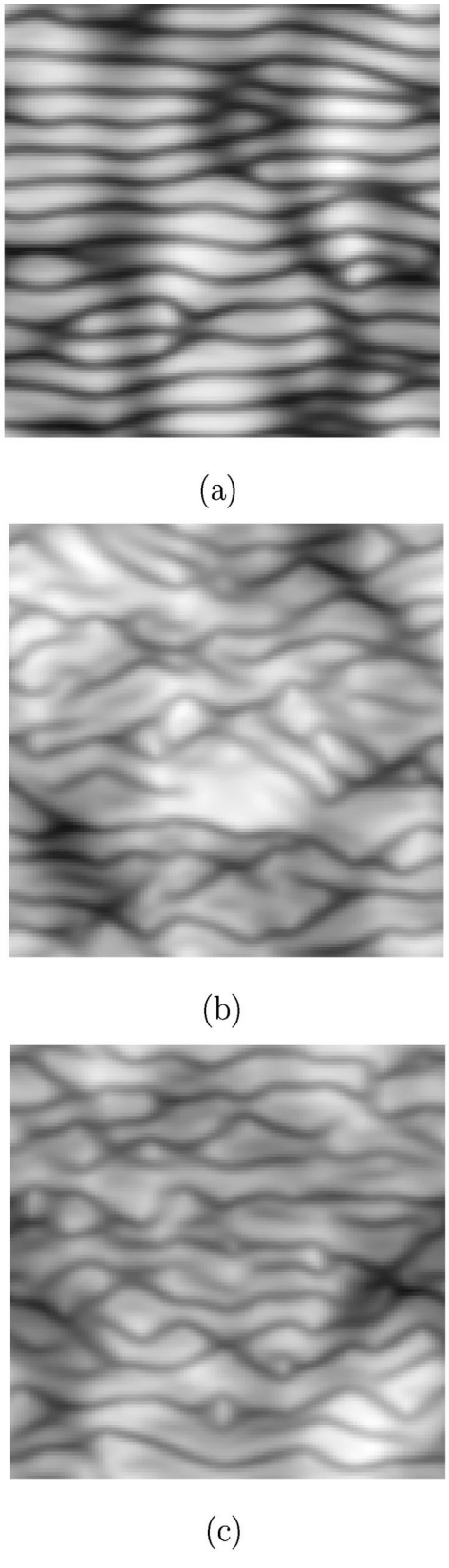

FIG. 2. Snapshots of a solution of Eq. (16) with $\delta_1=0$ and $\delta_2=1$ at (a) $T=40$, (b) $T=100$, and (c) $T=600$. The system size is 128×128 with the periodic boundary condition.

the finite system size. This is very similar to that observed in Ref. [32], and the third derivative term does not seem to play an important role in the present case.

Case IV: $v_c^x<v_c^y<v$. In this case the evolution equation is the same form as in case III. Since v is near v_c^y, δ_1 is large and δ_2 is a large negative parameter. The pattern in a late

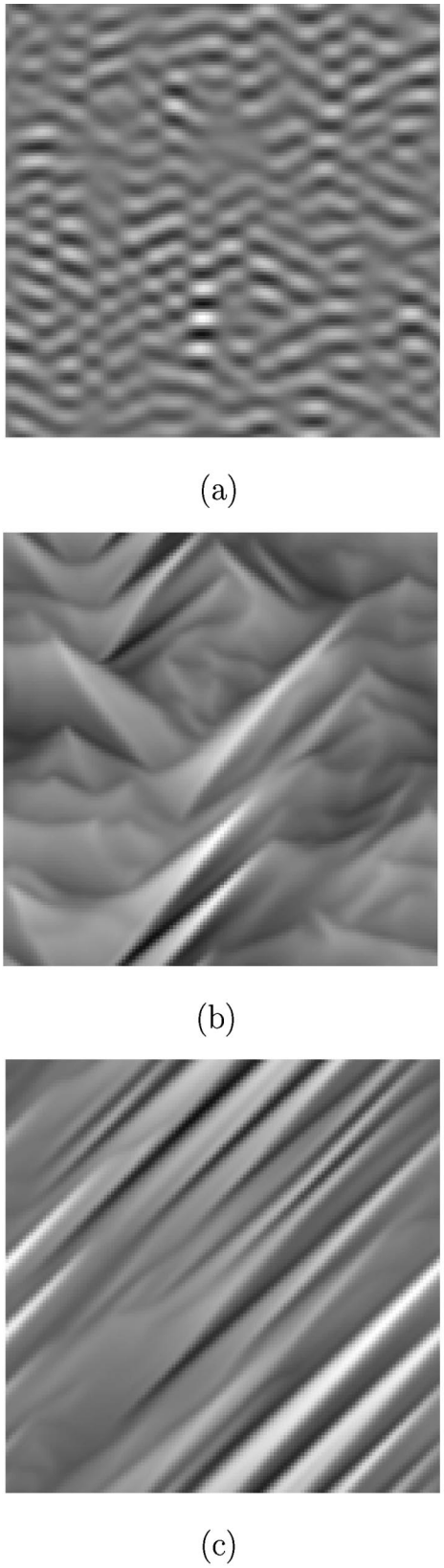

FIG. 3. Snapshots of a solution of Eq. (18) with $\delta_1=1$, $\delta_2=0.2$, and $\delta_3=1$ at (a) $T=20$, (b) $T=80$, and (c) $T=160$. The system size is 128×128 with the periodic boundary condition.

stage is a hill and valley structure similar to that in case III.

Figure 4 shows the time evolution of the surface width, for the pattern of Figs. 1–3, defined as

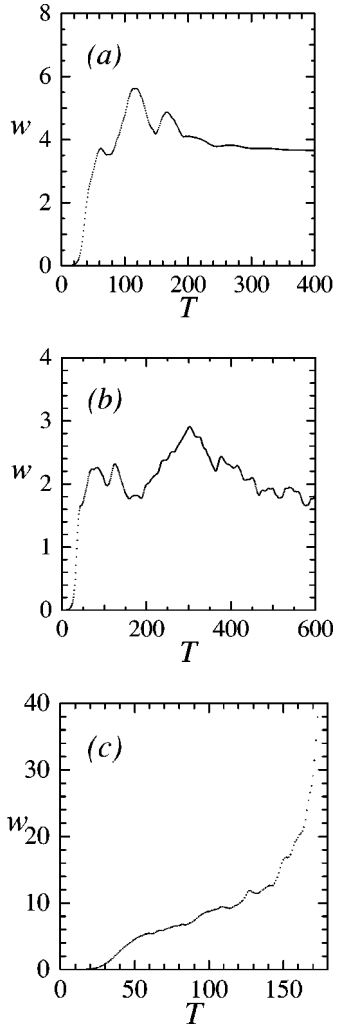

FIG. 4. Time evolution of the surface width, W, in (a) case I (Fig. 1), (b) case I (Fig. 2), and (c) case III (Fig. 3).

$$W=\sqrt{\frac{1}{L^2}\sum_{i,j}[H(i,j,T)-\overline{H}(T)]^2}, \tag{19}$$

where

$$\overline{H}(T)=\frac{1}{L^2}\sum_{i,j}H(i,j,T). \tag{20}$$

At the initial stage ($T\lesssim40$) the surface width increases rapidly as expected from the linear instability. Thus Fig. 1(a), Fig. 2(a), and Fig. 3(a) represent the surface patterns at the end of the exponential growth of the instability. In case I (Figs. 1 and 2) the linear instability occurs only in the y direction and the ripple structure parallel to the x direction appears. In case III (Fig. 3) the linear instability occurs both in the x and in the y direction. Since the wavelength of the most unstable mode is longer in the x direction, the undulation along the x axis appears more prominently. Nonlinearity dominates the pattern for $T\gtrsim40$. In case I the surface width saturates and a steady state seems to be realized, but the time evolution of the surface pattern and the width W is different with the third derivative term. When δ is large [Figs. 1 and 4(a)], after the growth and fluctuation, the width stays con-

stant and the ripple pattern becomes regular. When δ vanishes [Figs. 2 and 4(b)], on the other hand, the width is fluctuating perpetually and the pattern is chaotic. Thus the third derivative term, which breaks the inversion symmetry, is essential for the regular stable pattern. The behavior of the width is very different in case III [Figs. 3 and 4(c)]. In the early nonlinear stage ($40 \lesssim T \lesssim 150$), where the irregular striation is produced and two orthogonal regions coexist [Fig. 3(b)], the surface width increases gradually, which corresponds to slow growth of the domain. In the late stage ($150 \lesssim T$) one of the regions becomes dominant and the surface width increases very rapidly. Since this final stage of a single domain results from the finite system size, it is unphysical and will not be realized in real systems.

VI. DISCUSSION

In Si(111) vicinal surfaces, where step bunching is observed by many groups [21–24], the relevant parameters are estimated as $\tilde{\beta}=2.0\times10^{-10}$ J m^{-1} [33], $A=4.6\times10^{-30}$ J m [33], $D_s=1.8\times10^{-10}$ m^2/s [23], $x_s=1.3\times10^{-4}$ m [23], and $K=5.4\times10^{-4}$ m/s [23] at $T\approx900\,^{\circ}$C. When we use $\Omega=9\times10^{-20}$ m^2, $l=4\times10^{-7}$ m, the critical values of the instabilities are estimated to be $v_c^y\approx1.6\times10^{-17}$ m/s and $v_c^x\approx1.2\times10^{-11}$ m/s. Thus case II can hardly happen, and case I is much more likely than case III (case III may be realized with a small l). However, since the drift of adatoms is induced by an external field in many systems [34], all cases studied here may be realized in some other systems.

In Eq. (13) all the terms expected from the symmetry of the system appear. For simplicity, we have neglected several terms and studied the limited cases in this paper. The neglected terms may have some effect on the morphology we have found here. It is important to study more general cases, which will be done in the future.

ACKNOWLEDGMENTS

This work was performed as a part of the program ''Research for the Future'' of the Japanese Society for the Promotion of Science and was supported by a Grant-in-Aid from the Ministry of Education of Japan. The authors benefited from the Interuniversity Cooperative Research Program of the Institute for Materials Research, Tohoku University. M.U. would like to thank Laue-Langevin Institute, where part of the work was done, for hospitality.

[1] G. Ehrlich and F. G. Hudda, J. Chem. Phys. **44**, 1039 (1966).
[2] R. L. Schwoebel and E. J. Shipsey, J. Appl. Phys. **37**, 3682 (1966).
[3] G. S. Bales and A. Zangwill, Phys. Rev. B **41**, 5500 (1991).
[4] A. Pimpinelli, I. Elkinani, A. Karma, C. Misbah, and J. Villian, J. Phys.: Condens. Matter **6**, 2661 (1994).
[5] M. Sato and M. Uwaha, Phys. Rev. B **51**, 11 172 (1995).
[6] S. Stoyanov, Jpn. J. Appl. Phys., Part 1 **30**, 1 (1991).
[7] A. Natori, Jpn. J. Appl. Phys., Part 1 **33**, 3538 (1994).
[8] C. Misbah and O. Pierre-Louis, Phys. Rev. E **53**, R4318 (1996).
[9] M. Sato and M. Uwaha, J. Phys. Soc. Jpn. **65**, 1515 (1996).
[10] M. Sato and M. Uwaha, J. Phys. Soc. Jpn. **65**, 2146 (1996).
[11] M. Sato, M. Uwaha, and Y. Saito, Phys. Rev. Lett. **80**, 4233 (1998).
[12] D.-J. Liu and J. D. Weeks, Phys. Rev. B **57**, 14 891 (1998).
[13] S. Stoyanov and V. Tonchev, Phys. Rev. B **58**, 1590 (1998).
[14] M. Sato and M. Uwaha, J. Phys. Soc. Jpn. **67**, 3675 (1998).
[15] M. Kasu and N. Kobayashi, Appl. Phys. Lett. **62**, 1262 (1993).
[16] T. Fukui, J. Ishizaki, S. Hara, J. Motohisa, and H. Hasegawa, J. Cryst. Growth **146**, 183 (1995).
[17] H.-W. Ren, X.-W. Shen, and T. Nishinaga, J. Cryst. Growth **166**, 217 (1996).
[18] P. Tejedor, P. Šmilauer, C. Roberts, and B. A. Joyce, Phys. Rev. B **59**, 2341 (1998).
[19] M. Rost, P. Šmilauer, and J. Krug, Surf. Sci. **369**, 393 (1996).
[20] O. Pierre-Louis and C. Misbah, Phys. Rev. B **58**, 2276 (1998).
[21] A. V. Latyshev, A. L. Aseev, A. B. Krasilnikov, and S. I. Stenin, Surf. Sci. **213**, 157 (1989).
[22] Y. Homma, R. J. McClelland, and H. Hibino, Jpn. J. Appl. Phys., Part 2 **29**, L2254 (1990).
[23] Y.-N. Yang, E. S. Fu, and E. D. Williams, Surf. Sci. **356**, 101 (1996).
[24] A. V. Latyshev, H. Minoda, Y. Tanishiro, and K. Yagi, Surf. Sci. **401**, 22 (1998).
[25] D. Kandel and E. Kaxiras, Phys. Rev. Lett. **76**, 1114 (1996).
[26] The critical velocity v_c^x for an isolated step [10] is four times larger than the present one. Our condition here, $Kl/D_s \ll 1$, is opposite to that of Ref. [10], $K, l \to \infty$.
[27] $\zeta(x,y,t)$ is the variable obtained by taking the continuum limit of $\zeta_n(x,t)$, where y implies the step position of the ideal vicinal face. The fluctuation of surface height is given by $a\zeta(x,y,t)/l$ (a is the atomic step height, l is the average step distance).
[28] I. Bena, C. Misbah, and A. Valence, Phys. Rev. B **47**, 7408 (1993).
[29] Y. Kuramoto, Prog. Theor. Phys. **71**, 1182 (1984).
[30] D. E. Wolf, Phys. Rev. Lett. **67**, 1783 (1991).
[31] The change of the mesh size does not produce any appreciable change of the pattern.
[32] M. Rost and J. Krug, Phys. Rev. Lett. **75**, 3894 (1995).
[33] C. Alfonso, J. M. Bermond, J. C. Heyraud, and J. J. Métois, Surf. Sci. **262**, 371 (1992).
[34] H. Yasunaga and A. Natori, Surf. Sci. Rep. **15**, 205 (1992).